Hindawi Publishing Corporation
International Journal of Corrosion
Volume 2012, Article ID 162729, 11 pages
doi:10.1155/2012/162729

Research Article

Analysis of Short-Term Steel Corrosion Products Formed in Tropical Marine Environments of Panama

Juan A. Jaén,[1] Josefina Iglesias,[2] and Cecilio Hernández[2]

[1] *Departamento de Química Física, CITEN, Lab. No. 105, Edificio de Laboratorios Científicos-VIP, Universidad de Panamá, Panama, Panama*
[2] *Laboratorio de Análisis Industriales y Ciencias Ambientales, Universidad Tecnológica de Panamá, Panama, Panama*

Correspondence should be addressed to Juan A. Jaén, jjaen@ancon.up.ac.pa

Received 24 May 2012; Revised 20 June 2012; Accepted 4 July 2012

Academic Editor: Flavio Deflorian

A low-carbon steel A-36 and two conventional weathering steels A-588 and COR-420 exposed at four atmospheric test stations located in (i) Tocumen, an urban site near the Pacific Ocean, (ii) Sherman-Open, (iii) Sherman-Coastal, and (iv) Sherman-Breakwater on the Caribbean coast of Panama. Kinetics of the short-term atmospheric corrosion process and the relationship with exposure time and environmental characteristics of each site were investigated. The atmospheric exposure conditions, particularly the time of wetness, deposition of chloride, and the washing effect of contaminants on the metal surface by rain are of upmost importance in determining the corrosion behaviour and composition of rust. The corrosion products were mainly identified using room temperature and low temperature (80 K) Mössbauer spectroscopy, FTIR, and X-ray powder diffraction. In all samples, γ-FeOOH and α-FeOOH were the main constituents. Maghemite (γ-Fe_2O_3), magnetite (Fe_3O_4), and Akaganeite (β-FeOOH) were also identified.

1. Introduction

The study of the corrosion products which form on steel is of upmost importance since it renders valuable information for the understanding of corrosion mechanisms. Different types of steel corrode at rates determined by the environment. Corrosivity in marine tropical regions is usually regarded as extreme due to the high temperatures, time-of-wetness, high atmospheric contaminants (i.e., chlorides and SO_2), and other factors such as rainfall and winds.

There are several recent reports [1–10] on the corrosion products formed on mild and weathering steels in different marine regions. In Panama, there have been some systematic studies of atmospheric corrosion of steels. The studies of Southwell et al. [11, 12], the cooperative efforts of the Ibero-American Map of Atmospheric Corrosiveness (MICAT) [13], and the Project Anticorrosive Protection of Metals in the Atmosphere (PATINA) [14] are noteworthy. We also have investigated phase composition and other characteristics of the corrosion products of steel exposed to the tropical climate of Panama [15–18]. In this paper, the updated corrosion results are reported for carbon and weathering steel coupons, after a short-term exposure at different locations in Panama. An attempt is also made to correlate with corrosion data and meteorological and pollution parameters. Corrosion products were characterized by means of Mössbauer spectroscopy. Powder X-ray diffraction and infrared spectroscopy were used as complementary techniques. Mössbauer spectroscopy is especially suitable for studying steel corrosion due to its capability of identifying and quantifying the frequently found amorphous or noncrystalline phases of rust [19–22].

2. Materials and Methods

The mild steel (A-36) and weathering steels (A-588 and CSN COR 420) used in this study have been described elsewhere [18]. Their chemical composition is presented in Table 1. Coupons of 150 mm × 100 mm were used for atmospheric exposure. After blasting, cleaning, and degreasing with acetone, they were exposed, on inert racks, for prolonged

Table 1: Chemical composition of the studied steels.

Type of steel	Composition (mass %)					
	C	Cu	Mn	P	Si	Cr
A-36	0.150 ± 0.004	<0.01	0.42	0.20	0.24	<0.01
A-588	0.163 ± 0.002	0.36	0.75	0.10	0.23	0.18
COR 420	0.099 ± 0.002	0.27	0.55	0.023	0.20	0.37

Table 2: Starting date of exposure to the atmosphere.

Test site	Type of steel		
	A-36	A-588	COR 420
Tocumen	01/30/07	01/30/07	07/24/07
Sherman-Open	02/02/07	02/02/07	07/23/07
Sherman-Coastal	02/02/07	02/02/07	07/23/07
Sherman-Breakwater	01/31/07	01/31/07	07/23/07

periods. Panama is a tropical country, very humid and warm, with temperatures averaging 27°C all year long. Panama effectively experiences two seasons: namely, wet season and dry season. During the dry season (from the middle of December through the end of April) there is little or no precipitation; however in the wet season (from May to the beginning December) there is frequent and heavy precipitations.

Four test sites were used for atmospheric exposure. One at an urban test site in Tocumen (T) (9°4′2″N 79°24′16″W), Panama city, Pacific coast, and three other test sites in the tropical marine environment of Fort Sherman, Caribbean coast, Fort Sherman-Open (SO) (9°21′43″N 79°57′16″W), Coastal (SC) (9°22′19″N 79°57′2″W), and Breakwater site (SB) (9°22′25″N 79°56′50″W). The Breakwater site is a splash zone, thus there are a high amount of air-borne salt particles. Taking advantage of existing facilities, the samples were exposed at 45° to the horizontal in the Tocumen site and at 30° in the Sherman sites, as has been done in other works [13, 18]. Vera et al. [23] demonstrated that the exposure angle has some influences in the corrosion rate and the morphology of the rust, but with no effect on rust composition. The program of exposure is given in Table 2. Exposure of steels A-36 and A-588 started during dry season, whereas exposure of steel COR 420 started during the rainy season. This schedule was used because of a delay in arrival of materials to the laboratory. Corrosion results going back three years and rust characterization samples resulting from one year of testing are presented.

The atmosphere at each site was characterized from meteorological and atmospheric pollution data [24]. The average annual environmental parameters and ISO classifications are shown in Table 3. After exposure, corrosion rates (corrosion penetration p) were calculated from weight losses according to standard methods [25].

The corrosion products were characterized by XDR using Cu (K_α) radiation with a Bruker D8 Advance diffractometer, equipped with a detector angle Vantek 2000 at the Materials Institute of Universidad Autónoma de México (UNAM). IR spectra were recorded using a Nicolet Avatar 360 FTIR spectrometer. The resolution of the spectra was $4\,cm^{-1}$. Mössbauer spectra (MS) were recorded using a conventional spectrometer of constant acceleration with a $^{57}Co(Rh)$ source of nominal activity of 10 mCi (370 MBq). A closed-cycle cryostat (CCS 850 Janis) was employed for low temperature measurements. Calibrations were done with a standard α-iron foil absorber at room temperature. The Mössbauer data was evaluated with the Recoil software (University of Ottawa, Canada) using Voigt base fitting.

3. Results and Discussion

In general, after 3 months of exposure, most of the samples had their surface totally covered by brownish-orange rust. Weathering steels were slightly darker than mild steel. Most of the specimens at the Tocumen, Sherman-Open, and Sherman-Coastal sites had a good appearance of rust on both sides (the skywards facing side and the side facing the floor), but the later showed irregularities, and a nonuniform distribution of the rust, besides tracks of the route of corrosion liquid.

The samples exposed to the atmosphere at Sherman-Breakwater site had thicker corrosion product layers of dark chocolate colour, completely covering the steel substrate. In fact, the steel was totally corroded by the edges and exfoliates with relative ease. Sections were easily detached, exposing very dark and adherent rust in the central part of the specimen, which we denominated internal rust.

3.1. Corrosivity of Exposure Stations. As can be seen in Figure 1, the rust layer had a parabolic growth trend at the Tocumen and Sherman-Open stations, but for the Breakwater station, a linear growth behaviour was noted. The situation is more complex in the Coastal station, in which linear behaviour was observed for steels A-36 and COR 420, while steel A-588 showed a parabolic behaviour. It is sometimes difficult to differentiate between parabolic and linear behaviours with short-time exposures.

The corrosion rates ($\mu m\,y^{-1}$) obtained in the different exposure stations from tests going back two years are given in Table 4. It can be ascertained that corrosion rates are moderate at the Tocumen, Sherman-Open, and Sherman-Coastal stations. SO_2 deposition is not an important parameter in the aggressiveness of the test sites, thus corrosion can be linked to the deposition rate of chlorides. The amount of Cl^- deposited changed slightly between the Tocumen, Sherman-Open, and Sherman-Coastal stations, with a tendency to decrease along with the decrease in distance from shore, as expected. In steels A-36 and A-588, there is a trend that shows corrosion rate increase going from the Tocumen site, to the Sherman-Open and Sherman-Coastal sites. The Sherman sites have similar levels of chloride deposition rates (few $mgCl^-\,m^{-2}d^{-1}$). In the case of Sherman-Breakwater, the incidence of chlorides is substantial, increasing the values of corrosion rates and corrosion to all steels. It is interesting to note that in the dry season there is a higher deposition rate of chlorides. Some authors have reported [26–28] that deposition of chlorides depends on several factors, which include wind direction, wind speeds, rainfall, and distance

Table 3: Corrosivity at test stations based on environmental data during one year of exposure.

Test site	Distance from seashore (m)	Cl^{-1} (mg·m²/d)	SO_2 (mg·m²/d)	Time of wetness %	Classification of the environment ISO 9223	Corrosion class (ISO)
Tocumen	5000	11.7	4.0	55.3	$S_1P_0\tau_4$	C_3
Fort Sherman-Open	600	22.9	3.8	66.3	$S_1P_0\tau_5$	C_4
Fort Sherman-Coastal	50	29.0	3.9	66.3	$S_1P_0\tau_5$	C_4
Fort Sherman-Breakwater	3	1490.0	4.3	66.3	$S_3P_0\tau_5$	$>C_5$

Table 4: Two year results of the corrosion rates ($\mu m\, y^{-1}$).

Exposure time (months)	Tocumen			Sherman-Open			Sherman-Coastal			Sherman-Breakwater		
	A-36	A-588	COR 420	A-36	A-588	COR 420	A-36	A-588	COR 420	A-36	A-588	COR 420
3	22.1	33.3	63.7	31.6	37.2	51.2	47.3	52.7	67.1	1011.4	801.0	177.9
6	41.8	38.8	48.0	33.9	44.5	55.0	42.5	42.3	67.1	963.0	664.2	358.6
9	38.1	39.1	34.1	36.8	37.4	29.3	37.0	36.0	44.6	771.0	504.3	456.6
12	38.5	35.2	38.3	42.2	36.6	39.8	48.9	40.9	42.6	718.8	469.3	473.1
24	24.4	37.2	19.6	26.7	22.2	17.5	40.2	29.9	—	654.6	561.8	523.6

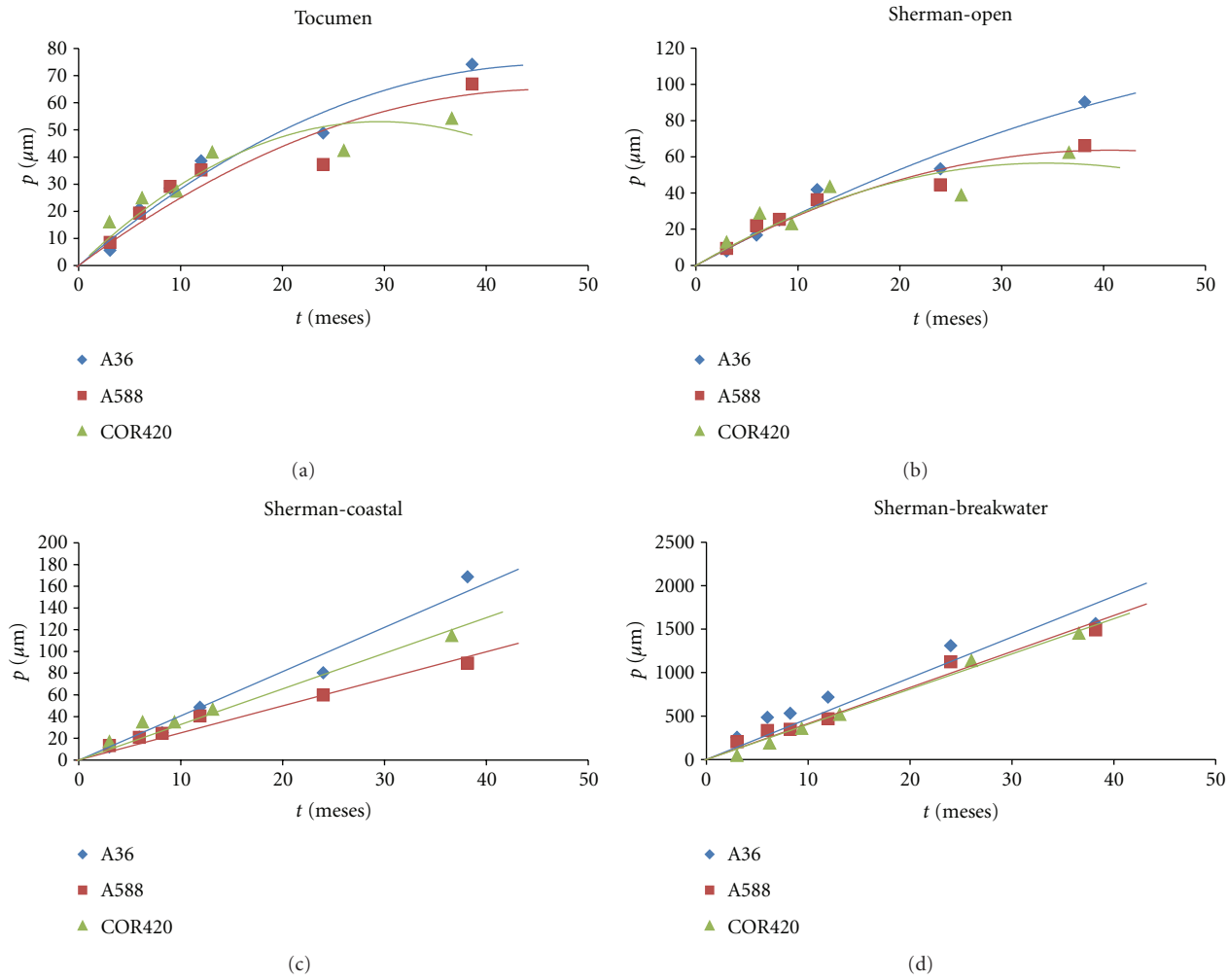

Figure 1: Penetration as a function of exposure time of the steels.

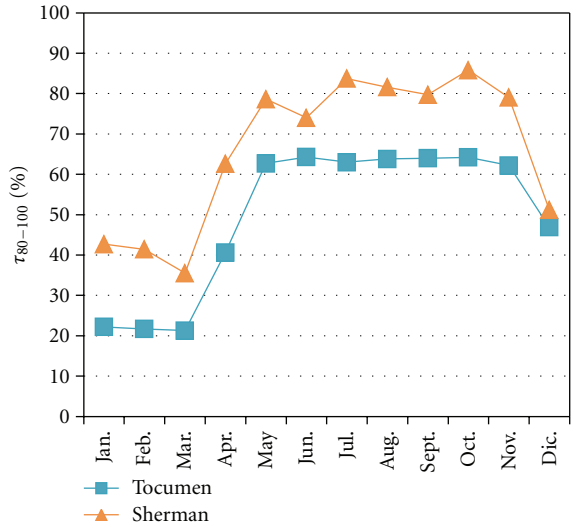

Figure 2: Time of wetness (RH 80%–100%) at the Tocumen in Sherman areas.

to shore. Deposition rates of chlorides in marine sites are usually in the range between 15 and 1500 $mg \cdot m^{-2} \cdot d^{-1}$ [26]. Our results from Breakwater station are much higher than usual, which is consistent with other places in the Caribbean [26, 27].

Even though it is not entirely clear, because of the outliers in the weight loss measurements, it seems that there is a transitional behaviour, particularly for steel COR 420; so that there is a different corrosion rate trend before and after a transition time (ca. 6 to 9 months). Before transition the corrosion rate is higher, afterwards there is a deceleration of corrosion. These types of changes in the kinetic of atmospheric corrosion have been reported for marine environments with high chloride content and high humidity [30]. The corrosion rates observed on weathering steel COR 420 at all test sites except Sherman-Breakwater are comparatively high in the initial phases of exposure, levelling off with time.

Exposure of the COR 420 steel began in the rainy season, while for steels A-36 and A-588 exposure started in the dry season. It is inferred that the conditions prevailing at the beginning of exposure determine the kinetics and the nature of corrosion products. Figure 2 shows that the time of wetness in the Sherman stations is larger at the Tocumen station. The greater period during which the metal surface of steel is covered by liquid films results in increased corrosion rates. On the other hand, the washing away of pollutants during the rainy season is the reason for the lower corrosion rate for COR 420 steel at the Sherman-Breakwater station. The deposition of pollutants combined with rainfall and wetting time is critical in corrosion rates. Data for the historical average annual rainfall in the Sherman area, shown in Figure 3, backs up this conclusion.

The rate of corrosion of a metal in a given environment, generally follows the Passano exponential equation $P = A \cdot t^n$ [31], where P represents the corroded amount expressed as penetration corroded (μm) or as weight loss, t is time in years, and A and n represent empirical constants. The value of the constant n is closely correlated to the progress of corrosion in subsequent years, and there may be three cases.

(a) If $n = 1$, the process occurs at constant rate, as there is a direct relationship between the exposure duration and penetration.

(b) If $n < 1$ would imply a decrease in corrosion rate.

(c) If $n > 1$ would imply an acceleration of the corrosion rate over time.

The value of n between 0.5 and 1.0 indicates that the corrosion products are not sufficiently protective. A value of less than 0.5 is obtained when the corrosion products quickly reach a parabolic growth, developing a barrier to the passage of aggressive agents, and considerably decreasing the corrosion rate.

The carbon steel A-36, the weathering steel A-588, and COR 420 follow the bilogarithmic relation at all sites of exposure, the results are presented in Table 5. It is interesting to note that the values of the intercepts are very similar between the Tocumen and Sherman-Open stations, with few significant differences, if the standard error in the measurement is considered. The values of n, determined as the slope of the bilogarithmic relation, indicate that the rust of carbon steel is not protective. Moreover, the weathering steels produce more protective rusts; the COR 420 steel being the steel which gives added protection. Therefore, systematically lower corrosion rates are observed in these steels after two years, when it begins to show the protective properties of weathering steel. The highest corrosion rates recorded at the Sherman-Breakwater station correlated with the highest category of air-borne chloride. The "n" values greater than 0.5 were observed at this exposure site revealing an acceleration of the diffusion process as a result of the rust detachment by erosion, flaking, cracking, and so forth.

3.2. Characterization of Corrosion Products. The IR analyses of the rust from samples at the different test sites were carried out. Figure 4 shows typical FTIR spectra of the corrosion products of the carbon and weathering steels exposed for three months, nine months, and one year. The characteristics bands at 1022 cm^{-1} and 746 cm^{-1} typical of lepidocrocite (γ-FeOOH) and at 885 cm^{-1} and 795 cm^{-1} typical of goethite (α-FeOOH) are observed on the rust layer formed on steels exposed at the Tocumen, Sherman-Open, and Sherman-Coastal stations. These are common phases found in steel corrosion products. In addition to these bands, there is one band at 1120 cm^{-1}, which Mendoza and Corvo [27] suggest may be due to the formation of a complex between the Fe and SO_2, but do not rule out the possibility that the band corresponds with feroxyhyte absorption (δ'-FeOOH) and/or lepidocrocite (γ-FeOOH). Given the low levels of SO_2 we have observed, it seems more likely that this band corresponds to one of the iron oxyhydroxides. In some cases intensity higher than expected [32] is observed, indicating the contribution of amorphous feroxyhyte (δ'-FeOOH), which has reported a broad and strong Fe-OH bending at 1110 cm^{-1}. The band at 1635 cm^{-1} corresponds to the

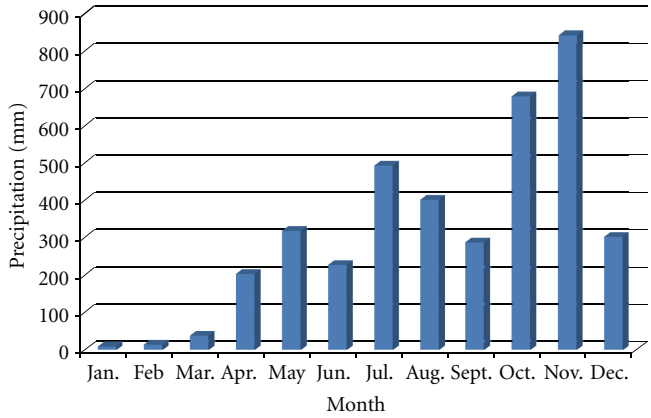

Figure 3: Data of the historical average annual rainfall in the Sherman area [29].

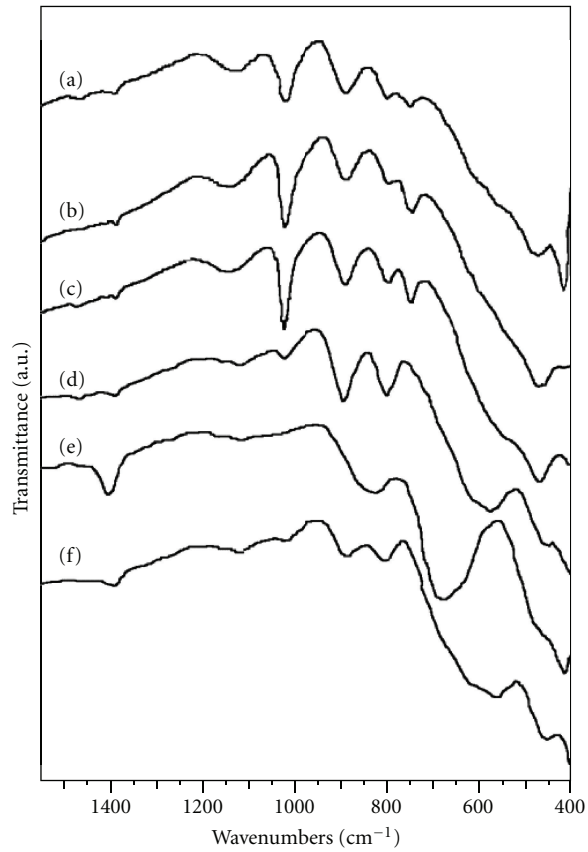

Figure 4: Fourier transformed infrared spectra of rusts formed at (a) Tocumen site A-588 for 6 months, (b) Sherman-Coastal site A-36 for 3 months, (c) Sherman-Open site COR 420 for 3 months, (d) Sherman-Breakwater site COR 420 for 1 year, and internal rusts formed at (e) Sherman-Breakwater rust A-588 for 1 year (f) Sherman-Breakwater rust COR 420 for 1 year.

Table 5: Summary of the results of the log-log plot of corrosion versus time.

log-log parameter	Tocumen			Sherman-Open			Sherman-Coastal			Sherman-Breakwater		
	A-36	A-588	COR420	A-36	A-588	COR420	A-36	A-588	COR420	A-36	A-588	COR420
A	30.04	29.06	32.6	32.59	30.92	31.90	42.23	36.53	40.67	726.40	556.50	395.70
n	0.92	0.73	0.47	0.92	0.71	0.55	0.95	0.76	0.56	0.72	0.82	1.37

bending vibration mode of H_2O, from which is inferred that these rust products contain molecular water adsorbed. The FTIR spectra obtained from the COR 420 rust, in addition to the bands of lepidocrocite and goethite, show that a shoulder band is located at 558 cm^{-1}, which is attributed to the maghemite.

The spectra for the A-36, A-588, and COR 420 steels exposed at Sherman-Breakwater site, also showed the typical bands of lepidocrocite and goethite. The lepidocrocite appear with low intensities in the FTIR spectra of the A-36 and A-588 steels, but with significant intensities in the sample of COR 420 steel. In the COR 420 sample the band is not only very intense, but also quite sharp, thus this phase should be well-crystallized in this rust. In addition, all samples clearly show a band at 578 cm^{-1} (see Figure 4(d)) approximately corresponding to magnetite (Fe_3O_4). The relative amounts of goethite and magnetite appear to increase with exposure duration at the expense of lepidocrocite phase.

In the product formed in the internal parts of panels exposed at Sherman-Breakwater (i.e., rust removed from the flaked parts corresponding to the interior of the panels) of steels A-36 and A-588, akaganeite (β-FeOOH) could be identified by the strong and broad bands at approximately 830 cm^{-1} and 667 cm^{-1} (see e.g., Figure 4(e)). In the COR 420 steel absorptions at 884 cm^{-1} and 799 cm^{-1}, corresponding to the goethite (α-FeOOH), plus an intense band 577 cm^{-1}, typical of magnetite (Fe_3O_4), could clearly be observed, as shown in Figure 4(f).

The formation of akaganeite is also observed in the rust in the internal flaking parts of the A-36 and A-588 steels. Curiously, akaganeite was not clearly detected in the COR 420 steels by FTIR, but instead magnetite was observed. We assume that this is due to the rain washing of chloride contaminants during the exposure in the rainy season. Considering the predominant phases in the internal parts of the COR 420 steels specimens were composed of goethite and magnetite, it follows that the washing of these samples in the early stages of exposure limits the possibilities of reaching the critical levels of chlorides required for the formation of akaganeite, as proposed by Santana Rodríguez et al. [33]. The magnetite is formed by the reducing conditions prevailing inside the flaked steel, where oxygen diffusion is limited. The formation of magnetite and akaganeite is most probably favoured in the presence of Cl^-, by the transformation of lepidocrocite and ferric species of FeOOH.

In order to establish whether or not there were differences in the corrosion products between the skyward and downward facing sides, we also undertook a comparative analysis using infrared FT-IR spectroscopy. There were no significant differences in the nature of the compounds in the rust, but there were differences in the relative amounts of phases in some cases. In previous work [34], which studied the corrosion products of carbon steel A-36 exposed to the weather in the tropical marine environment of Fort Sherman on the Caribbean coast of Panama, and compared the results with those obtained in an urban site in Panama city, with the help of X-ray diffraction, it was concluded that basically there are differences in the characteristics of particle size between the skyward facing and downward facing sides. No differences in the nature of the corrosion products on both sides were reported working with carbon steel A-36 at the station in Panama city.

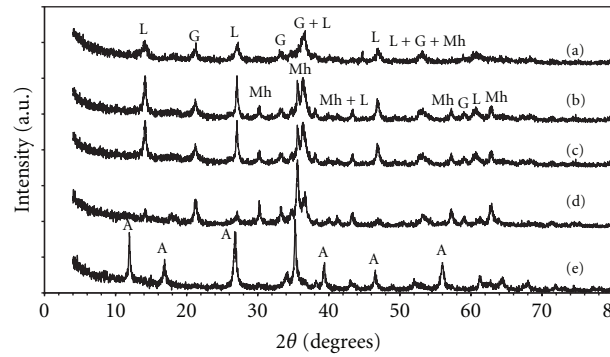

Figure 5: XRD patterns of some characteristic samples. (a) Tocumen site A-588 for 3 months, (b) Sherman-Open site A-588 for 3 months, (c) Sherman-Breakwater site A-588 for 1 year, (d) Sherman-Breakwater site COR 420 for 1 year, and internal rusts formed at (e) Sherman-Breakwater rust A-588 for 1 year. A, G, L, and Mh stand for akaganeite, goethite, lepidocrocite, and maghemite, respectively.

X-ray powder diffraction pattern for all samples was recorded to confirm the identification of the phases present due to corrosion. The X-ray diffraction patterns corroborated with the previous FTIR analysis, although the relative intensities of the diffraction peaks detected were changed from coupon to coupon. However, the predominance of lepidocrocite or goethite based only on X-ray diffraction results was difficult to determine, since XRD only allows the analysis of crystalline constituents. Some phases like magnetite (Fe_3O_4) or maghemite (γ-Fe_2O_3) could not be differentiated by XRD measurements due to their similar crystalline structure. This oxide was always found in considerable proportions in the rust from weathering steels COR 420, particularly in Sherman-Breakwater samples. The presence of akaganeite, as expected for saline environments with high amounts of chlorides, was detected in a few samples by the presence intensities at 2θ angles of 11.8° and 55.7°. A discussion of the implications of these outcomes was presented previously [18] and will be extended later using Mössbauer results. Representative X-ray diffraction patterns are shown in Figure 5. Characteristics peaks associated with goethite (G), lepidocrocite (L), maghemite (Mh), and akaganeite (A) are shown.

Mössbauer analysis of the phase composition of the corrosion products of mild steel (A-36) and two weathering steels (A-588 and COR 420) formed after 3-months exposure to the tropical marine atmosphere of Panama has been reported elsewhere [18]. The results show that amorphous or crystallized iron oxyhydroxides goethite α-FeOOH and lepidocrocite γ-FeOOH are early corrosion products. Maghemite γ-Fe_2O_3 and magnetite Fe_3O_4 were also identified in the most aggressive conditions. The formation of akaganeite β-FeOOH was observed when chlorides were occluded within the rust.

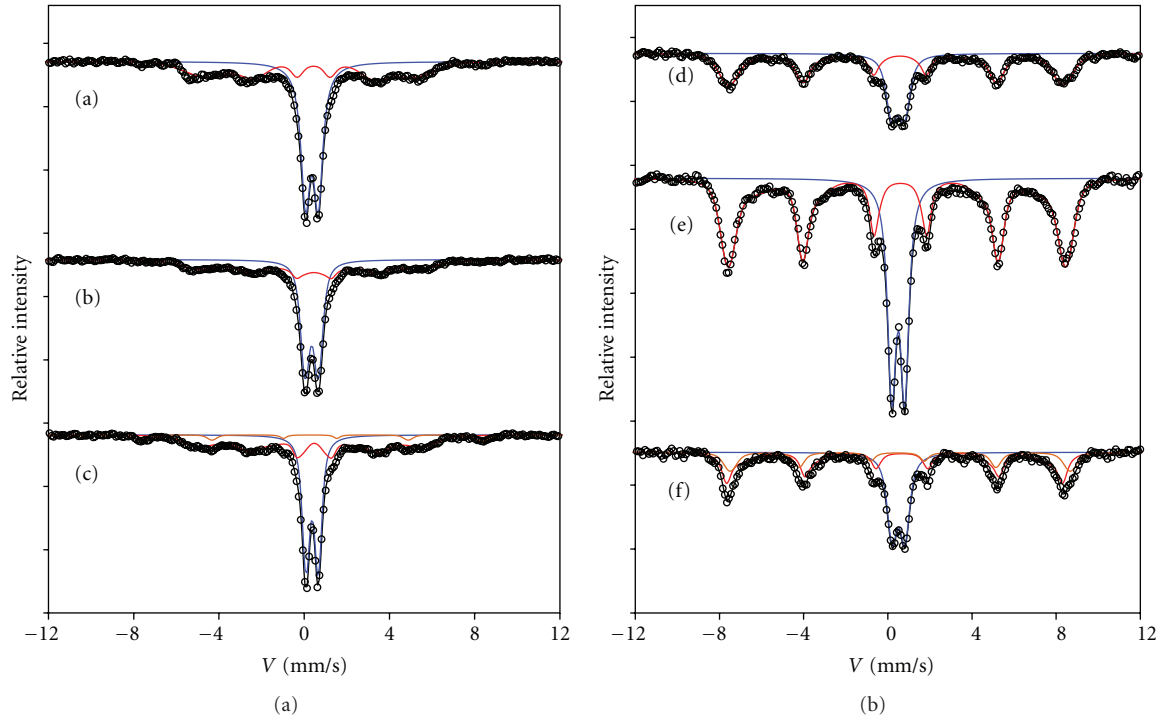

Figure 6: Transmission Mössbauer spectra of rust of mild steel A-36 and weathering steels formed after one year exposure at Tocumen site at 295 K: (a) A-36, (b) A-588, and (c) COR 420, and at 80 K: (d) A-36, (e) A-588, and (f) COR 420.

Figures 6 and 7 show the Mössbauer spectra of skyward corrosion products of the carbon steel and weathering steels coupons after 1 year of exposure at the Tocumen and Sherman-Breakwater sites. Table 6 summarizes the Mössbauer results as relative abundance determined basically from the 80 K spectra; but in the case of α-FeOOH, both room temperature and 80 K data were used because of the temperature dependence of the Mössbauer spectrum profile of this phase. α-FeOOH particles of >15 nm are magnetic at 298 K, while superparamagnetic α-FeOOH of <15 nm displays a doublet at room temperature and a magnetic sextet at 80 K [22]. Mössbauer spectrum of superparamagnetic α-FeOOH with particles <8 nm remains a doublet at 80 K [34, 35].

The fitting parameters indicate that the corrosion products of most samples contain γ-FeOOH, magnetic α-FeOOH, and superparamagnetic α-FeOOH, several also have γ-Fe_2O_3. The fitting of magnetic α-FeOOH at 298 K showed collapsing magnetic profile due to a broad distribution with the average of the hyperfine magnetic field ranging from 25.0–32.2 T, showing the poor crystallinity of this phase, particularly in the samples from Tocumen, Sherman-Open, and Sherman-Coastal. It is noteworthy that, at a given exposure duration, the relative concentration of superparamagnetic α-FeOOH is mostly larger for carbon steel A-36 and weathering A-588, compared to weathering steel COR 420. Rust formed at Sherman-Coastal station also contains magnetic γ-Fe_2O_3, phase which has also been observed in similar previous studies [15–17]. On one hand, superparamagnetic α-FeOOH has been shown to be important for the formation of the protective layer on weathering steels [4, 22]; on the other hand, Oh et al. [35] have linked the formation of magnetic γ-Fe_2O_3 and large particles of α-FeOOH to the increase of corrosion rates of different steels. Therefore, there is a lower corrosion rate for steel A-36 and A-588 exposed to mild corrosion conditions of Tocumen and Sherman-Open sites, compared with those exposed in Sherman-Coastal, which is attributed to superparamagnetic α-FeOOH. It is possible that γ-Fe_2O_3 enhances the corrosion rate by forming nonprotective patina. The presence of large particle of γ-Fe_2O_3 in all steel COR 420 coupons can be caused by the high humidity exposure existed during the rainy season. It is known that periods of wet-dry cycles, with long wet and shor-dry periods, form large fractions of γ-Fe_2O_3 [22]. Other factors like composition of the steel and the morphology should be examined.

Disregarding the type of steel, the Mössbauer results show that magnetic γ-Fe_2O_3 is always formed in large quantities at the Sherman-Breakwater site. This indicates that the harsh environmental condition of contamination by chlorides promotes the formation of γ-Fe_2O_3. The washing effect on the corrosion rate is noticed during the rainy season, affecting the composition of corrosion products due to the natural elimination of chloride contamination from the oxide layer. This may explain why there was a relatively low amount of γ-Fe_2O_3 in the COR 420 corrosion products of steel exposed at the Sherman-Breakwater site, and lower corrosion rate observed for the A-36 and A-588 steels.

Large amounts of magnetite and akaganeite are produced in the inner layer corrosion products from steels

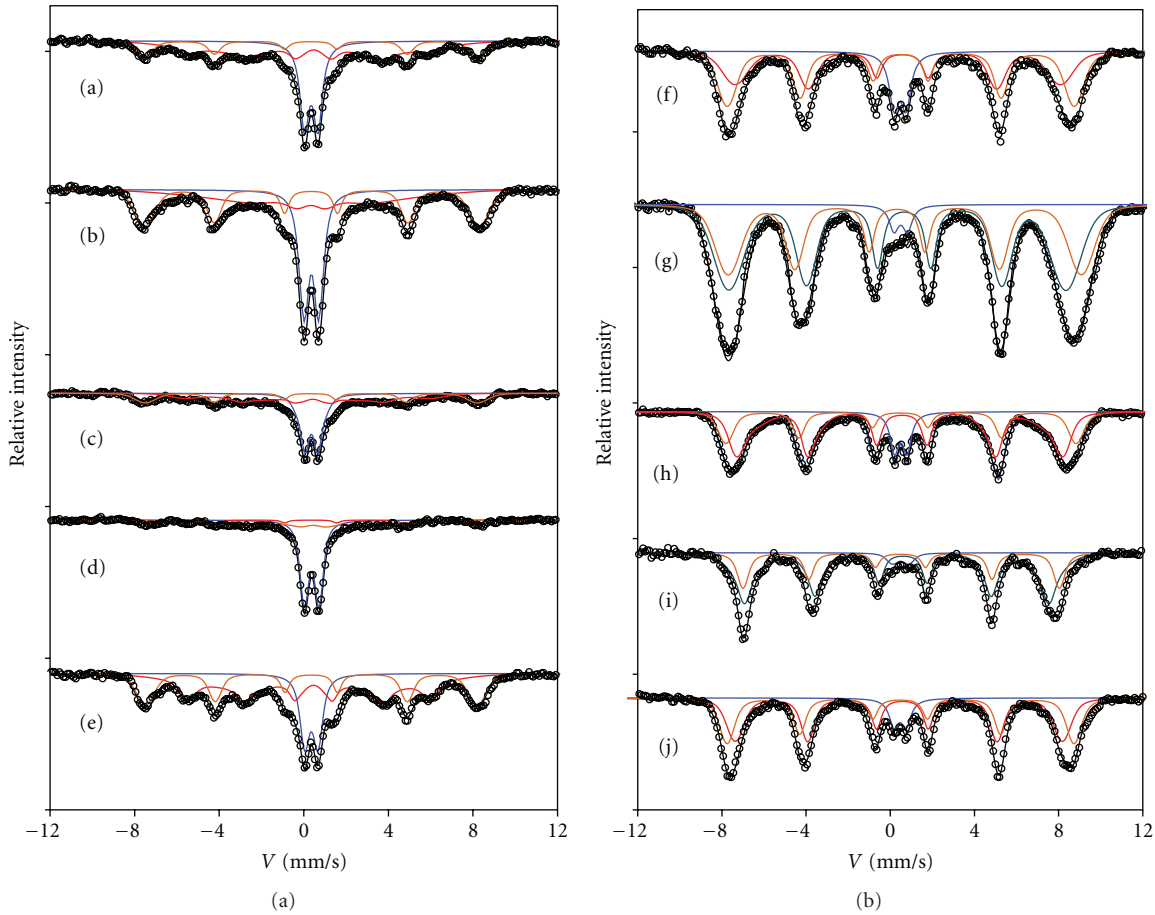

Figure 7: Transmission Mössbauer spectra of rust of mild steel A-36 and weathering steels formed after one year exposure at Sherman-Breakwater site at 295 K: (a) A-36, (b) internal rusts A-36, (c) A-588, (d) internal rusts A-588, and (e) COR 420, and at 80 K: (f) A-36, (g) internal rusts A-36, (h) A-588, (i) internal rusts A-588, and (j) COR 420.

exfoliated. This is due to the high chloride contamination that accumulates in the inner parts of the coupons, where salt is occluded. As we have already pointed out, β-FeOOH as corrosion product is typical of coastal areas that have high concentrations of chloride due to marine aerosols. It is presumed that β-FeOOH is formed instead of goethite and its presence may be related to the Fe_3O_4 in the rust, leading to high corrosion rates.

The differences in composition between the samples could be related to the conditions prevailing at the beginning of the exposure, giving different rates of corrosion, affecting the nature of corrosion products, and also to the composition of steels. The current results suggest that under severe chloride contamination, such as in the Sherman- Breakwater site, corrosion is controlled primarily by this pollutant and time of wetness, not the products of corrosion.

Protection ability is associated with corrosion products, alloying elements, exposure environment, and pollutants. In the initial stages of atmospheric corrosion, the formation of γ-FeOOH is predominant, but it further converts to goethite, in concordance with observations after long-term exposures [35, 36]. Actually, there might be favourable conditions for the formation of other corrosion products, such as maghemite, as previously pointed out. After a year, in the wet conditions of the atmosphere of Panama, the layer structure in rust is still loose, not providing protection. The corrosion rate data suggest that after three year's exposure, the dense corrosion-protective patina of fine rust particles in the weathering steels barely starts forming. Thus, the proposed protective ability index (PAI) of the rust layer [37] and the classification of the corrosion rate of the nonprotective rust layer [38] may be used with caution as these criteria were defined from long-term exposures. In addition, as indicated by Cook [22], it is magnetic goethite, that is, large particle goethite >15 nm exhibiting magnetic sextet at 298 K in the Mössbauer spectrum, that is the component that can be identified in the XRD patterns. As we obtained the fractions of the components by Mössbauer, for the rust to be a protective coating, the suggested value of more than two in weathering steel should be used for the ratio (α_m/γ^*), where α_m and γ^* are the mass ratio of crystalline α-FeOOH, and the total of γ-FeOOH, β-FeOOH and spinel-type iron oxide, respectively. This ratio in the skyward samples is less than 2 in all samples, but the ratio (β-FeOOH + spinel-type iron oxide)/(β-FeOOH + γ-FeOOH + spinel-type iron oxide), was less than 0.5 in samples exposed

Table 6: Mössbauer relative concentrations (%) for corrosion products after exposure at tests sites for six months and one year.

Exposure time	Type of steel	Exposure site	α-FeOOH (m)[1]	α-FeOOH (s)[2]	α-FeOOH Total	γ-FeOOH	γ-Fe_2O_3 /Fe_3O_4	β-FeOOH
6 months	A-36	Tocumen	23.6	41.6	65.2	34.8	—	—
		Sherman-Open	36.7	35.6	72.3	27.6	—	—
		Sherman-Coastal	25.3	41.1	66.4	33.6	—	—
		Sherman-Breakwater	38.8	44.7	83.5	16.5	—	—
	A-588	Tocumen	38.0	27.7	65.7	34.3	—	—
		Sherman-Open	48.4	17.4	65.8	34.2	—	—
		Sherman-Coastal	43.3	17.2	60.5	39.5	—	—
		Sherman-Breakwater	51.0	28.8	79.8	9.9	10.3	—
	COR 420	Tocumen	44.2	15.6	59.8	32.1	8.1	—
		Sherman-Open	30.4	12.4	42.8	37.1	20.1	—
		Sherman-Coastal	31.6	7.0	38.6	35.2	26.1	—
		Sherman-Breakwater	—	21.9	20.5	12.2	65.9	—
		Sherman-Breakwater I*	40.0	7.0	47.0	10.9	19.0	23.0
1 year	A-36	Tocumen	43.8	23.0	66.8	33.2	—	—
		Sherman-Open	31.3	22.5	53.8	39.5	6.7	—
		Sherman-Coastal	46.7	7.5	54.2	37.9	7.9	—
		Sherman-Breakwater	20.7	19.3	40	13.6	47.0	—
		Sherman-Breakwater I*	—	—	—	3.4	40.7	55.9
	A-588	Tocumen	48.3	15.0	63.3	36.7	—	—
		Sherman-Open	37.8	16.0	53.8	39.5	6.7	—
		Sherman-Coastal	23.6	20.8	44.4	40.6	15.0	—
		Sherman-Breakwater	33.5	25.8	59.3	11.6	29.1	—
		Sherman-Breakwater I*	—	—	—	—	29.0	71.0
	COR 420	Tocumen	32.1	8.9	41.0	37.0	22.0	—
		Sherman-Open	21.9	11.6	33.5	37.5	29.0	—
		Sherman-Coastal	28.1	14.9	43.0	39.3	17.7	—
		Sherman-Breakwater	38.9	11.5	50.4	8.6	41.0	—

* Corrosion product from the inner layer of flaked simple.
[1] α-FeOOH (m): magnetic goethite (>15 nm) exhibiting magnetic sextet at 298 K.
[2] α-FeOOH (s): superparamagnetic goethite (<15 nm) exhibiting superparamagnetic doublet at 298 K and magnetic sextet at 80 K.

to mild corrosion conditions of the Tocumen, Sherman-Open, and Sherman-Coastal sites, whereas it was more than 0.5 in Sherman-Breakwater. Hence, the rust obtained after one year exposure under mild conditions should be nonprotective but inactive, whereas the rust from Sherman-Breakwater is active, showing high corrosion rates.

4. Conclusions

(i) The atmospheric corrosion behaviour of samples of carbon steel A-36 weathering steels A-588, and COR 420 exposed to the humid tropical weather at different sites in Panama proceeded according to the well-known bilogarithmic law for weight loss. This process could be linked to the high chloride content and high relative humidity. The difference in corrosion of steels at the various sites with mild conditions was small, with a variation of A from 30 to 42 and n from 0.5 to 1.0 (using corrosion depth in mm, and years as time). The difference was large for the Sherman-Breakwater station, a highly contaminated site with chlorides, with A values varying from 396 to 726 and n values from 0.7 to 1.4. The corrosion rate observed on weathering steel COR 420 is high in the initial phases of exposure (rainy season) levelling off with time. There is a transitional behaviour at the Sherman-Breakwater site for weathering steel COR-420, with different corrosion rates before and after 6 to 9 months.

(ii) There is a strong correlation between compositions of rust formed in dependence of the atmospheric exposure conditions, particularly the time of wetness, deposition of chloride, and the washing effect of contaminants on the metal surface by rain. The dominant phases after short-term exposure were amorphous or crystalline oxyhydroxides such as lepidocrocite (γ-FeOOH) and goethite (α-FeOOH). Maghemite (γ-Fe_2O_3) and magnetite (Fe_3O_4) were

also found. Akaganeite (β-FeOOH) was identified as prominent component in the most aggressive conditions, with high chlorine amounts, and occluded within the rust.

(iii) The rust obtained after one year exposure is nonprotective, inactive in the mild conditions of the Tocumen, Sherman-Open, and Sherman-Coastal sites, but active in the rust from the Sherman-Breakwater site.

Acknowledgment

The authors are thankful to Secretaría Nacional de Ciencia, Tecnología e Innovación (Panamá), for financial help through the Project FID06-227, SENACYT, 2006.

References

[1] Q. C. Zhang, J. S. Wu, J. J. Wang, W. L. Zheng, J. B. Chen, and A. B. Li, "Corrosion behavior of weathering steel in marine atmosphere," *Materials Chemistry and Physics*, vol. 77, pp. 603–608, 2002.

[2] R. A. Antunes, R. A. CI, and D. L. Araújo de Faria, "Characterization of corrosion products formed on steels in the first months of atmospheric exposure," *Materials Research*, vol. 6, no. 3, pp. 403–408, 2003.

[3] K. Asami and M. Kikuchi, "In-depth distribution of rusts on a plain carbon steel and weathering steels exposed to coastal-industrial atmosphere for 17 years," *Corrosion Science*, vol. 45, no. 11, pp. 2671–2688, 2003.

[4] D. C. Cook, "Application of Mössbauer spectroscopy to the study of corrosion," *Hyperfine Interactions*, vol. 153, no. 1–4, pp. 61–82, 2004.

[5] T. Kamimura, S. Hara, H. Miyuki, M. Yamashita, and H. Uchida, "Composition and protective ability of rust layer formed on weathering steel exposed to various environments," *Corrosion Science*, vol. 48, no. 9, pp. 2799–2812, 2006.

[6] W. Han, G. Yu, Z. Wang, and J. Wang, "Characterisation of initial atmospheric corrosion carbon steels by field exposure and laboratory simulation," *Corrosion Science*, vol. 49, no. 7, pp. 2920–2935, 2007.

[7] Y. Li, "Mössbauer effect of rust layer formed on steel in different marine corrosion zones," *Corrosion*, vol. 63, no. 9, pp. 850–856, 2007.

[8] Y. C. Sica, E. D. Kenny, K. F. Portella, and D. F. Campos Filho, "Atmospheric corrosion performance of carbon steel, galvanized steel, aluminum and copper in the North Brazilian coast," *Journal of the Brazilian Chemical Society*, vol. 18, no. 1, pp. 153–166, 2007.

[9] F. Corvo, T. Perez, L. R. Dzib et al., "Outdoor-indoor corrosion of metals in tropical coastal atmospheres," *Corrosion Science*, vol. 50, no. 1, pp. 220–230, 2008.

[10] J. G. Castaño, C. A. Botero, A. H. Restrepo, E. A. Agudelo, E. Correa, and F. Echeverría, "Atmospheric corrosion of carbon steel in Colombia," *Corrosion Science*, vol. 52, no. 1, pp. 216–223, 2010.

[11] A. L. Alexander, B. W. Forgenson, H. W. Mumdt, C. R. Southwell, and S. J. Thompson, "Corrosion of metals in tropical environments, part-1 test methods used and result obtained for pure metals and a structural steel," NRL Report 4929, Washington, DC, USA, 1957.

[12] C. R. Southwell, B. W. Forgeson, and A. L. Alexander, "Corrosion of metals in tropical environments, part-2 atmospheric corrosion of ten structural steels," NRL Report 5002, Washington, DC, USA, 1957.

[13] M. Morcillo, E. Almeida, B. Rosales, J. Uruchurtu, and M. Marrocos, Corrosión y Protección de Metales en las Atmósferas de Iberoamérica. Parte I: Mapas de Iberoamérica de Corrosividad Atmosférica (Red Temática MICAT, XV.1/CYTED) Madrid: CYTED, 1999.

[14] M. Morcillo, E. Almeida, F. Fragata, and Z. Panossian, Corrosión y Protección de Metales en las Atmósferas de Iberoamérica. Parte II: Protección Anticorrosiva de Metales en las Atmósferas de Iberoamérica (Red Temática PATINA, XV.D/CYTED) Madrid: CYTED, 2002.

[15] J. A. Jaén and B. Fernández, "Mössbauer spectroscopy study of steel corrosion in a tropical marine atmosphere," *Electrochimica Acta*, vol. 34, no. 6, pp. 885–886, 1989.

[16] J. A. Jaén, M. S. De Villalaz, L. De Araque, and A. De Bósquez, "Kinetics and structural studies of the atmospheric corrosion of carbon steels in Panama," *Hyperfine Interactions*, vol. 110, no. 1-2, pp. 93–99, 1997.

[17] J. A. Jaén, M. S. de Villalaz, L. de Araque, C. Hernández, and A. de Bósquez, "Study of the corrosion products formed on carbon steels in the tropical atmosphere of Panama," *Revista de Metalurgia*, pp. 32–37, 2003.

[18] J. A. Jaén, A. Muñóz, J. Justavino, and C. Hernández, "Characterization of initial atmospheric corrosion of conventional weathering steels and a mild steel in a tropical atmosphere," *Hyperfine Interactions*, vol. 192, no. 1–3, pp. 51–59, 2009.

[19] H. Leidheiser Jr. and S. Musić, "The atmospheric corrosion of iron as studied by Mössbauer spectroscopy," *Corrosion Science*, vol. 22, no. 12, pp. 1089–1096, 1982.

[20] A. K. Singh, T. Ericsson, L. Häggström, and J. Gullman, "Mössbauer and x-ray diffraction phase analysis of rusts from atmospheric test sites with different environments in Sweden," *Corrosion Science*, vol. 25, no. 10, pp. 931–945, 1985.

[21] N. R. Furet, C. Haces, F. Corvo, C. Díaz, and J. Gomez, "Corrosion rate determination using57Fe Mössbauer spectra of corrosion products of steel," *Hyperfine Interactions*, vol. 57, no. 1–4, pp. 1833–1838, 1990.

[22] D. C. Cook, "Spectroscopic identification of protective and non-protective corrosion coatings on steel structures in marine environments," *Corrosion Science*, vol. 47, no. 10, pp. 2550–2570, 2005.

[23] R. Vera, B. M. Rosales, and C. Tapia, "Effect of the exposure angle in the corrosion rate of plain carbon steel in a marine atmosphere," *Corrosion Science*, vol. 45, no. 2, pp. 321–337, 2003.

[24] ISO 9223, *Corrosion of Metal and Alloys—Classification of Corrosivity of Atmospheres*, International Standards Organization, Geneva, Switzerland, 1992.

[25] ISO 9226, *Corrosion of Metals and Alloys. Method for Determination of Corrosion Rate of Standard Specimens for the Evaluation of Corrosivity*, International Standards Organization, Geneva, Switzerland, 1991.

[26] F. Corvo, C. Haces, N. Bethancourt et al., "Atmospheric corrosivity in the Caribbean area," *Corrosion Science*, vol. 39, no. 5, pp. 823–833, 1997.

[27] A. R. Mendoza and F. Corvo, "Outdoor and indoor atmospheric corrosion of carbon steel," *Corrosion Science*, vol. 41, no. 1, pp. 75–86, 1999.

[28] M. Morcillo, B. Chico, L. Mariaca, and E. Otero, "Salinity in marine atmospheric corrosion: its dependence on the wind

regime existing in the site," *Corrosion Science*, vol. 42, no. 1, pp. 91–104, 2000.

[29] ETESA—Empresa de Transmisión Eléctrica, S.A. Hidrometeorología de ETESA, 2011, http://www.hidromet.com.pa.

[30] Y. Ma, Y. Li, and F. Wang, "The atmospheric corrosion kinetics of low carbon steel in a tropical marine environment," *Corrosion Science*, vol. 52, no. 5, pp. 1796–1800, 2010.

[31] R. F. Passano, "The Harmony of Outdoors Weatherfng Steels," in *Proceedings on the Outdoor Wheathering of Metals and Metalic Coating*, Philadelphia, Pa, USA, 1934.

[32] A. Raman, B. Kuban, and A. Razvan, "The application of infrared spectroscopy to the study of atmospheric rust systems-I. Standard spectra and illustrative applications to identify rust phases in natural atmospheric corrosion products," *Corrosion Science*, vol. 32, no. 12, pp. 1295–1306, 1991.

[33] J. J. Santana Rodríguez, F. J. Santana Hernández, and J. E. González González, "XRD and SEM studies of the layer of corrosion products for carbon steel in various different environments in the province of Las Palmas (The Canary Islands, Spain)," *Corrosion Science*, vol. 44, no. 11, pp. 2425–2438, 2002.

[34] J. A. Jaén Osorio, De Gracia de Araque Ld. A Study of the Corrosion Products on Carbon Steel Exposed in the Caribbean Coast of Panama. In Congreso Latinoamericano de Corrosión LATINCORR, 2006/9 Congreso Iberoamericano de Corrosión y Protección/6 Congreso de Corrosión NACE Latinoamericano, Fortaleza, Brazil, 2006.

[35] S. J. Oh, D. C. Cook, S. J. Kwon, and H. E. Townsend, "Studying the atmospheric corrosion behavior of weathering steels at a mild marine environment," *Hyperfine Interactions*, vol. 4, pp. 49–54, 1999.

[36] S. J. Oh, D. C. Cook, and H. E. Townsend, "Atmospheric corrosion of different steels in marine, rural and industrial environments," *Corrosion Science*, vol. 41, no. 9, pp. 1687–1702, 1999.

[37] M. Yamashita, H. Miyuki, Y. Matsuda, H. Nagano, and T. Misawa, "The long term growth of the protective rust layer formed on weathering steel by atmospheric corrosion during a quarter of a century," *Corrosion Science*, vol. 36, no. 2, pp. 283–299, 1994.

[38] S. Hara, T. Kamimura, H. Miyuki, and M. Yamashita, "Taxonomy for protective ability of rust layer using its composition formed on weathering steel bridge," *Corrosion Science*, vol. 49, no. 3, pp. 1131–1142, 2007.